

Supporting Information of
The Optimal Electronic Structure for High-Mobility 2D Semiconductors:
Exceptionally High Hole Mobility in 2D Antimony

Long Cheng, Chenmu Zhang, Yuanyue Liu*
 Texas Materials Institute and Department of Mechanical Engineering
 The University of Texas at Austin, Austin, TX, 78712
[*yuanyue.liu@austin.utexas.edu](mailto:yuanyue.liu@austin.utexas.edu)

Computational Methods

We perform first-principles calculations using the Quantum Espresso Package¹ with the SG15 Optimized Norm-Conserving Vanderbilt pseudopotentials (SG15 ONCV Potentials)²⁻⁴ and the Perdew-Burke-Ernzerhof⁵ (PBE) exchange-correlation functional. The kinetic energy cutoffs for wave functions and charge density are set to 60 and 240 Ry, respectively. The atomic coordinates are optimized using a $36 \times 36 \mathbf{k}$ mesh until the magnitude of the force acting on each atom becomes less than 0.0001 Ry/Bohr. The spin-orbit coupling is included for As, Sb, and Bi.

To obtain the mobility, we first use density functional perturbation theory⁶ (DFPT) to calculate the electron-phonon coupling (EPC) strengths (g) for $9 \times 9 \mathbf{k}$ (electron wavevector) points and $9 \times 9 \mathbf{q}$ (phonon wavevector) points, where three (six for the spin-orbit case) p orbitals per atom is used for the initial Wannier projection⁷. Then the g for $300 \times 300 \mathbf{k}$ and $300 \times 300 \mathbf{q}$ points are obtained using the interpolation approach as implemented in the EPW code⁸. We use the Gaussian function with a broadening of 5 meV to account for the Delta function in Eq. 2. The lower boundary for the phonon frequency in the electron-phonon coupling calculations is set as 5 cm⁻¹ (corresponds to 0.62 meV). We find that $300 \times 300 \mathbf{k}$ and \mathbf{q} are sufficient to converge the mobility values.

The contribution of an electronic state $i\mathbf{k}$ to the mobility is characterized as:

$$p(i\mathbf{k}) = \frac{\tau(i\mathbf{k})v^2(i\mathbf{k}) \left| \frac{\partial f_0}{\partial E_{i\mathbf{k}}} \right|}{\sum_i \int_{BZ} f_0 d\mathbf{k}}, \quad (S1)$$

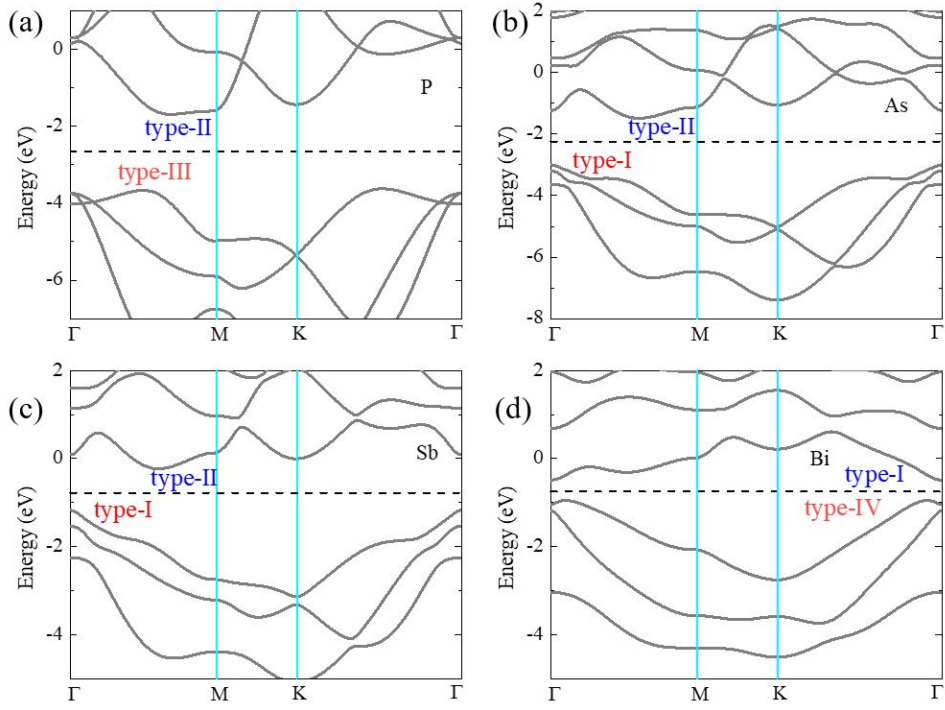


Figure S1 Electronic band structures of the group-15 hexagonal 2D materials. The Fermi levels are shown by the black dashed lines. The band types near the band edge states are labelled.

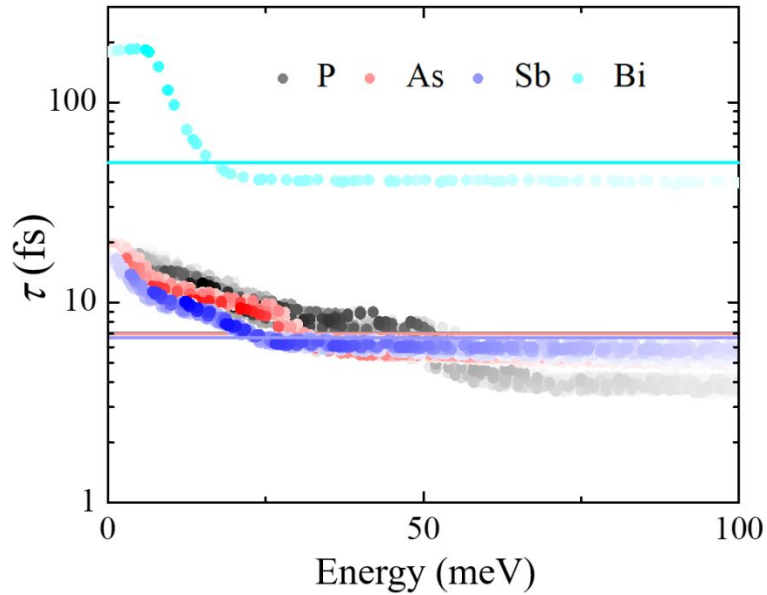


Figure S2 Relaxation time τ of the electrons (shown by dots), and the “average relaxation time” $\bar{\tau}$ (shown by lines). The energy of the conduction band minimum is set to be zero. The color shade of the τ represents the contribution of the corresponding electronic state to the mobility.

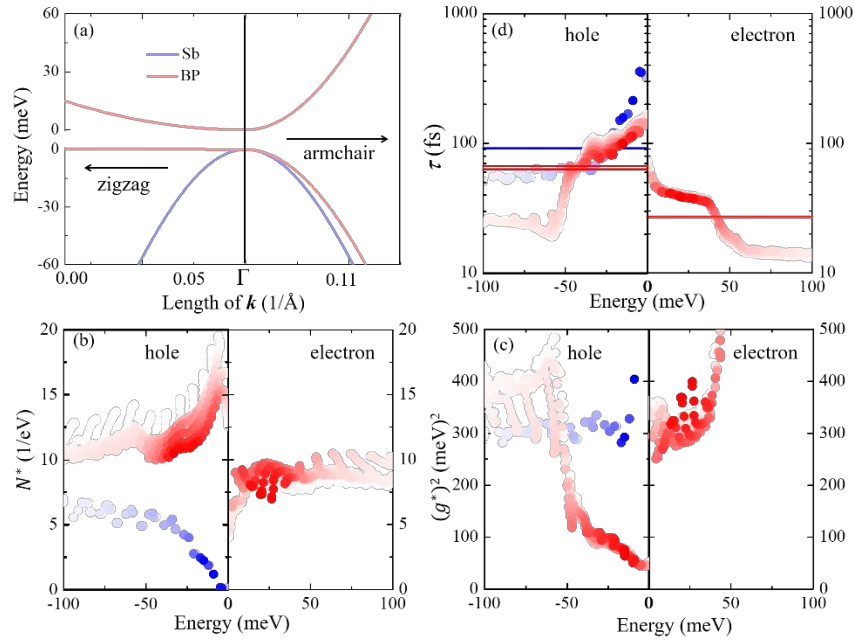


Figure S3 (a) Band structure of monolayer black phosphorus (BP) and Sb. (b-d) Comparison of effective number of states (b), effective EPC strength (c), and relaxation time (d), between the BP (electrons and holes) and Sb (holes). The average relaxation times are shown in (d) as horizontal lines. The color strength represents the contribution of the corresponding electronic state to the mobility.

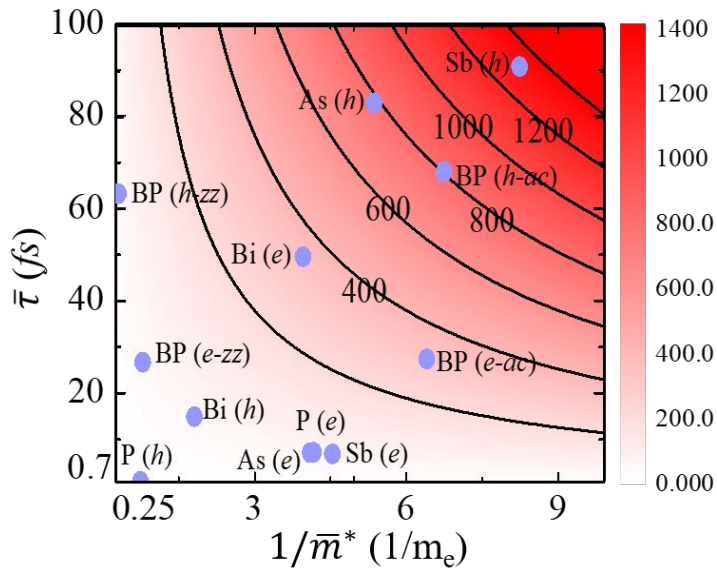


Figure S4 Carrier mobility as a function of “average effective mass” \bar{m}^* and “average relaxation time” $\bar{\tau}$ (see the main text for definition). Note that the BP has an anisotropic structure (rectangular) while others have isotropic (hexagonal) structures.

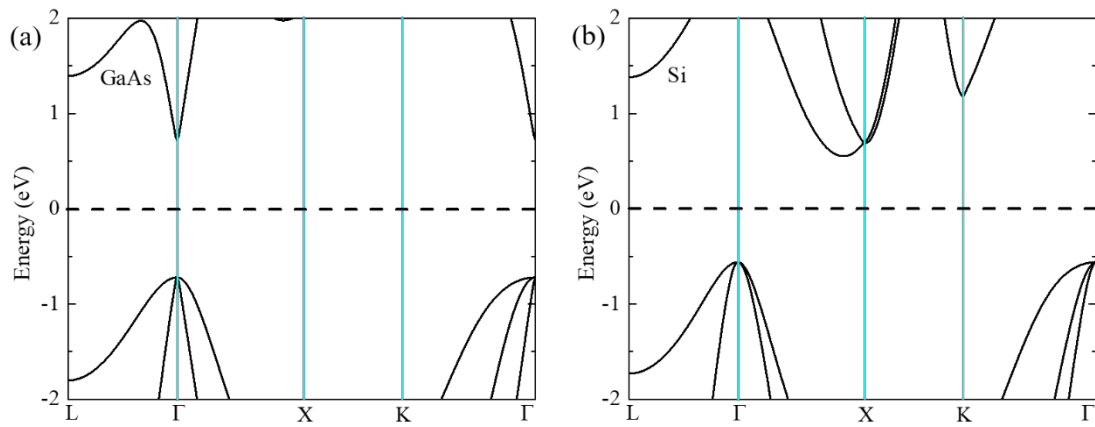


Figure S5 Electronic structures of GaAs (a), and Si (b), calculated using PBE functional with the band gap shifted to be experimental value.

Table S1 The effective mass m^* of the band edge state, the “average effective mass” \bar{m}^* , and the “average relaxation time” $\bar{\tau}$ of the group-15 2D hexagonal materials.

	holes			electrons		
	$m^*(m_e)$	\bar{m}^*	$\bar{\tau}$ (fs)	$m^*(m_e)$	\bar{m}^*	$\bar{\tau}$ (fs)
	(m_e)			(m_e)		
2D P	1.3613	1.3400	0.7	0.2432	0.2383	7.1
2D As	0.1549	0.1850	83.2	0.2353	0.2420	7.0
2D Sb	0.1050	0.1204	91.2	0.2162	0.2187	6.7
2D Bi	0.4443	0.5489	14.8	0.2343	0.2507	49.7

Table S2 Comparison between experimentally measured and theoretically calculated (using Boltzmann transport theory with scattering rates obtained from first principles) electron mobility at room temperature for Si, GaAs, and monolayer MoS₂. Note that for monolayer MoS₂, we choose the experiments that use four-terminal or Hall measurements so that the contact resistance is subtracted.

	Experimental ($\text{cm}^2\text{V}^{-1}\text{s}^{-1}$)	Calculation ($\text{cm}^2\text{V}^{-1}\text{s}^{-1}$)
Si (e)	1300 ~ 1450, Ref. ⁹⁻¹¹	1366, Ref. ¹²
GaAs (e)	8200 ~ 8900, Ref. ¹³⁻¹⁹	8899, Ref. ²⁰
Monolayer MoS ₂ (e)	11 ~ 165, Ref. ²¹⁻²³	176, this work

Reference

1. Paolo, G.; Stefano, B.; Nicola, B.; Matteo, C.; Roberto, C.; Carlo, C.; Davide, C.; Guido, L. C.; Matteo, C.; Ismaila, D.; Andrea Dal, C.; Stefano de, G.; Stefano, F.; Guido, F.; Ralph, G.; Uwe, G.; Christos, G.; Anton, K.; Michele, L.; Layla, M.-S.; Nicola, M.; Francesco, M.; Riccardo, M.; Stefano, P.; Alfredo, P.; Lorenzo, P.; Carlo, S.; Sandro, S.; Gabriele, S.; Ari, P. S.; Alexander, S.; Paolo, U.; Renata, M. W., QUANTUM ESPRESSO: a modular and open-source software project for quantum simulations of materials. *J. Phys. Condens. Matter* **2009**, *21* (39), 395502.
2. Hamann, D. R., Optimized norm-conserving Vanderbilt pseudopotentials. *Phys. Rev. B* **2013**, *88* (8), 085117.
3. Scherpelz, P.; Govoni, M.; Hamada, I.; Galli, G., Implementation and Validation of Fully Relativistic GW Calculations: Spin–Orbit Coupling in Molecules, Nanocrystals, and Solids. *J. Chem. Theory Comput.* **2016**, *12* (8), 3523-3544.
4. Schlipf, M.; Gygi, F., Optimization algorithm for the generation of ONCV pseudopotentials. *Comput. Phys. Commun.* **2015**, *196*, 36-44.
5. Perdew, J. P.; Burke, K.; Ernzerhof, M., Generalized Gradient Approximation Made Simple. *Phys. Rev. Lett.* **1996**, *77* (18), 3865-3868.
6. Giustino, F., Electron-phonon interactions from first principles. *Rev. Mod. Phys.* **2017**, *89* (1), 015003.
7. Mostofi, A. A.; Yates, J. R.; Lee, Y.-S.; Souza, I.; Vanderbilt, D.; Marzari, N., wannier90: A tool for obtaining maximally-localised Wannier functions. *Comput. Phys. Commun.* **2008**, *178* (9), 685-699.
8. Poncé, S.; Margine, E. R.; Verdi, C.; Giustino, F., EPW: Electron–phonon coupling, transport and superconducting properties using maximally localized Wannier functions. *Comput. Phys. Commun.* **2016**, *209*, 116-133.
9. Canali, C.; Jacoboni, C.; Nava, F.; Ottaviani, G.; Alberigi-Quaranta, A., Electron drift velocity in silicon. *Phys. Rev. B* **1975**, *12* (6), 2265-2284.
10. Norton, P.; Braggins, T.; Levinstein, H., Impurity and Lattice Scattering Parameters as Determined from Hall and Mobility Analysis in n-Type Silicon. *Phys. Rev. B* **1973**, *8* (12), 5632-5653.
11. Sze, S. M.; Ng, K. K., *Physics of semiconductor devices*. John wiley & sons: 2006.
12. Poncé, S.; Margine, E. R.; Giustino, F., Towards predictive many-body calculations of phonon-limited carrier mobilities in semiconductors. *Phys. Rev. B* **2018**, *97* (12), 121201.
13. Rode, D. L., Electron Mobility in Direct-Gap Polar Semiconductors. *Phys. Rev. B* **1970**, *2* (4), 1012-1024.
14. Rode, D. L.; Knight, S., Electron Transport in GaAs. *Phys. Rev. B* **1971**, *3* (8), 2534-2541.
15. Blakemore, J. S., Semiconducting and other major properties of gallium arsenide. *J. Appl. Phys.* **1982**, *53* (10), R123-R181.
16. Hicks, H. G. B.; Manley, D. F., High purity GaAs by liquid phase epitaxy. *Solid State Commun.* **1969**, *7* (20), 1463-1465.
17. Wolfe, C. M.; Stillman, G. E.; Lindley, W. T., Electron Mobility in High Purity GaAs. *J. Appl. Phys.* **1970**, *41* (7), 3088-3091.
18. Blood, P., Electrical Properties of \$n\$-Type Epitaxial GaAs at High Temperatures. *Phys. Rev. B* **1972**, *6* (6), 2257-2261.
19. Požela, J.; Reklaitis, A., Electron transport properties in GaAs at high electric fields. *Solid State Electron.* **1980**, *23* (9), 927-933.
20. Zhou, J.-J.; Bernardi, M., Ab initio electron mobility and polar phonon scattering in GaAs. *Phys. Rev. B* **2016**, *94* (20), 201201.
21. Lembke, D.; Allain, A.; Kis, A., Thickness-dependent mobility in two-dimensional MoS₂ transistors. *Nanoscale* **2015**, *7* (14), 6255-6260.
22. Baugher, B. W. H.; Churchill, H. O. H.; Yang, Y.; Jarillo-Herrero, P., Intrinsic Electronic Transport Properties of High-Quality Monolayer and Bilayer MoS₂. *Nano Lett.* **2013**, *13* (9), 4212-4216.
23. Kang, J.; Liu, W.; Banerjee, K., High-performance MoS₂ transistors with low-resistance molybdenum contacts. *Appl. Phys. Lett.* **2014**, *104* (9), 093106.

